HERA Memo #105
Received: 5 Nov 2021

A COMPARISON OF S_{11} MEASUREMENTS, AUTOCORRELATIONS, AND ELECTROMAGNETIC MODELS OF THE HERA DISH+FEED: THE HEIGHT OF THE FEED ABOVE THE DISH

Jacqueline N. Hewitt, Bang D. Nhan, Daniel Riley, Scott B. C. Dynes
Richard F. Bradley, Nicolas Fagnoni, Daniel C. Jacobs, Eloy de Lera Acedo, Nima Razavi-Ghods
Lorena B. Aguirre, Justin Bracks, Suzannah A. Fraker
5 November 2021

ABSTRACT

We compare measurements of the S_{11} scattering parameter to electromagnetic models of the HERA antenna element. We consider three antenna models that vary in the degree to which they conform to the as-built configuration of the antenna, and we find that the predictions of S_{11} vs. frequency for the three models are significantly different. We further consider models in which we vary the height of the feed above the dish. We develop a goodness-of-fit metric for comparing the measurements to the models. We find that of the three different models for the antenna element, the one that most closely conforms to the construction of the antenna is clearly the best fit to the data, suggesting that S_{11} measurements are a good discriminator between models. We further find that the goodness-of-fit metric differentiates between models of the feed at different heights, and we find the best-fit height for each model. The best-fit heights agree with those measured in the field, except for a consistent offset of a few centimeters. This offset may be due to a bias caused by inaccuracies in the antenna model, errors in the zero point of the field measurements, or unmodeled motions of the feed (such as horizontal motion or tilt). The internal consistency of the fitted heights suggests that in principle S_{11} measurements could be used to measure feed heights in the field to a precision of about 2cm, if the source of bias could be understood and corrected. However, S_{11} measurements may not be practical during operations. We show that the frequency dependence of antenna autocorrelations on feed height is systematic and predictable, and thus might be used instead to infer feed height.

1. Introduction

Understanding the response of the HERA antenna to celestial signals is important for optimizing calibration and assessing systematic errors. The HERA dish+feed system is complicated, and we are using electromagnetic models of the antenna performance as a

framework for our understanding. An important step in the analysis is verifying that the electromagnetic models do indeed reproduce the response of the antenna. The electromagnetic simulations give models for a number of properties of the antenna, including antenna gain as a function of azimuth, elevation and frequency (beam patterns), and scattering parameters as a function of frequency. Ideally, the models would be verified through comparison to measurements of beam patterns and scattering parameters for real antenna in the field. Measurements of HERA and low-frequency SKA antenna beam patterns are difficult but are being explored; see, for example Nunhokee et al. (2020), de Lera Acedo et al. (2018), Jacobs et al. (2017), Neben et al. (2016). In this memo we focus instead on measurements of the S_{11} scattering parameter, a quantity that is relatively easy to measure with a Vector Network Analyzer (VNA). We also focus on one particular aspect of the dish+feed system: the height of the feed above the dish. The effect of feed motions relative to the dish is of considerable importance as the raising of feeds proceeds during commissioning, and as we seek to understand the source of non-redundancies in antenna calibration.

Electromagnetic models of the HERA dish+feed system, based on the antenna model developed by Fagnoni et al. (2021) have been calculated for a range of heights above the feed. The Fagnoni et al. nominal model is very detailed and computation of many "runs" of the model with different parameters is expensive. We therefore have also investigated simplifications to the model that reduce computing time. As a result, we have different sets of models, detailed and simplified, that can be compared. We have reason to believe that the detailed model will be a better predictor of antenna performance. Here we assess whether S_{11} measurements can distinguish between the different antenna models, and whether the measurements can in principle be used to determine feed height in the field. Since S_{11} measurements may not be practical during HERA operations, we also assess the effect of feed height variations on the antenna autocorrelation spectra.

In July and September 2018, members of the HERA-MIT and HERA-UVA groups carried out field measurements of the S11 antenna scattering parameter at the HERA test site at Galford Meadow in Green Bank, West Virginia. Participants in the July campaign were Lorena Aguirre, Justin Bracks, Richard Bradley, Suzannah Fraker, Jacqueline Hewitt, Bang Nhan, and Daniel Riley. Bang Nhan carried out the September campaign. This memo reports on a subset of those measurements, those that were carried out as the feed height above the dish was varied. A complete report of the all the measurements and their comparison to models is postponed for a future memorandum.

2. Antenna Measurements

A prototype version of the Vivaldi feed was built on-site at Green Bank; Figure 1 shows the feed on the ground facing the sky along with close-up views of the four-pin feed point assembly.

Fig. 1.— Left: A HERA Vivaldi feed, inverted for on-sky testing at Green Bank in July 2018. Center: Detail of the four-pin feed point assembly. Right: The assembly of the feed points, custom adaptor plate, and Macom HH-128 180-degree hybrid as a balun.

On 12 July 2018 a Vivaldi feed was raised above the HERA dish in Galford meadow as shown in Figure 2. A 50-Ohm coaxial cable approximately 50 meters in length carried signals from the feed points to an Anritsu MS2024A VNA. Calibration of the VNA-cable-balun response was done by attaching two calibration standards (each with open, short, load references) to the two-port input of the balun and carrying out the standard Anritsu VNA calibration sequence. As part of a series of measurements in we which explored changes in antenna response as properties of the system were varied, we took S11 measurements with the feed positioned at five different heights. Three of the heights were nominally at 3.53m, 4.91m, and 5.10m above the dish. The other two, for which we do not have measured positions, were between the 3.53m and 4.91m measurements. Repeated measurements at several of the heights were made, providing a basis for assessment of consistency.

On 22 September 2018 the feed was again raised, and further measurements were carried out (Nhan 2018). These measurements were done with an HP 8753D Network Analyzer, also with a dual-standard calibration procedure. Measurements were made at nominal heights of 4.83m, 4.93m, 5.04m, 5.16m, and 5.29m for the feed above the dish.

Feed heights were measured with a Bosch GLM40 laser rangefinder with its bottom

Fig. 2.— The Vivaldi feed on the HERA dish in Galford Meadow.

reference plane resting on the top of the concrete hub of the antenna. In July, the reference point on the feed used for the height measurement was 1.5cm from the fiducial reference point in the electromagnetic models. We measured the top surface of the concrete hub to be 8.3cm above the vertex on the inner surface of the dish. For comparison with the electromagnetic models, the nominal feed heights recorded in the field were corrected for the concrete hub thickness and, in the case of the July measurements, for the offset from the fiducial reference point. Table 1 summarizes these data.

For the analysis that follows, it is important to have an estimate of the S11 measurement error. During the July campaign, two measurements of S11 were taken one after the other, for the purpose of assessing the error. Figure 3 shows the difference between those two measurements. The standard deviations for the real and imaginary components are 0.00265 and 0.00243, respectively. We take $1/\sqrt{2}$ times the average of these to be the Anritsu VNA measurement error for one component (real or imaginary) of S_{11}: $\sigma_o = 0.00179$. During the September campaign, there were no repeated measurements of S_{11}, so we estimate the error by examining the root-mean-square variation about a polynomial fit. We chose a section of the spectrum that could be fit by a low-order polynomial fit (the first 50 channels, 50-68 MHz), and found that subtracting a third-order polynomial fit to the Anritsu VNA (July) data gave the same (within 10%) root-mean-square variation as the differencing of two successive measurements. Therefore, we fit a third-order polynomial in the same frequency range to the HP VNA (September) data and take $1/\sqrt{2}$ times the standard deviation to be the HP VNA measurement errors: $\sigma_o = 0.00146$. Figure 3 shows the data plotted on the polynomial fits.

In Figure 4 we plot the data after averaging together S11 measurements taken at the

Label	**Laser**	**Correction(cm)**	$\mathbf{h_{corr}}$ (m)	N_{meas}
J1	139in	8.3+1.5	3.63	3
J2	–	–	–	3
S1	4.83m	8.3	4.91	1
S2	4.93m	8.3	5.01	1
J3	–	–	–	3
J4	193.25in	8.3+1.5	5.01	2
S3	5.04m	8.3	5.12	1
J5	201in	8.3+1.5	5.20	3
S4	5.16m	8.3	5.24	1
S5	5.29m	8.3	5.37	1

Table 1: The ten feed heights for which S_{11} measurements were carried out. "Laser" refers to the laser distance measurement recorded in the field. "Correction" refers to the correction needed to align the measurements with the CST reference point: 8.3cm for the thickness of the concrete hub in Green Bank and 1.5cm for the thickness of the PVC supporting the feed. $h_{\mathbf{corr}}$ refers to the field height corrected for the difference in reference points between field measurements and the CST models; this is the height we refer to as the "set height" when we compare measurements and models. For the labeling, "J" refers to a measurement taken in July, and "S" refers to a measurement taken in September. N_{meas} is the number of measurements that were averaged.

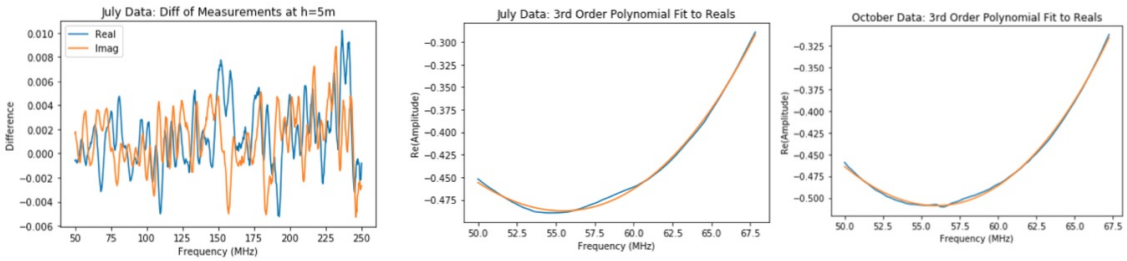

Fig. 3.— Data used for VNA measurement error estimation. Left: Difference between two successive S11 measurements at the same height for the July (Anritsu VNA) data; real and imaginary parts. Center: 3rd-order polynomial fit to the July data in the frequency range 50-68 MHz. Right: 3rd-order polynomial fit to the September (HP VNA) data in the same frequency range.

same feed height. The number of measurements that went into each average are listed in Table 1.

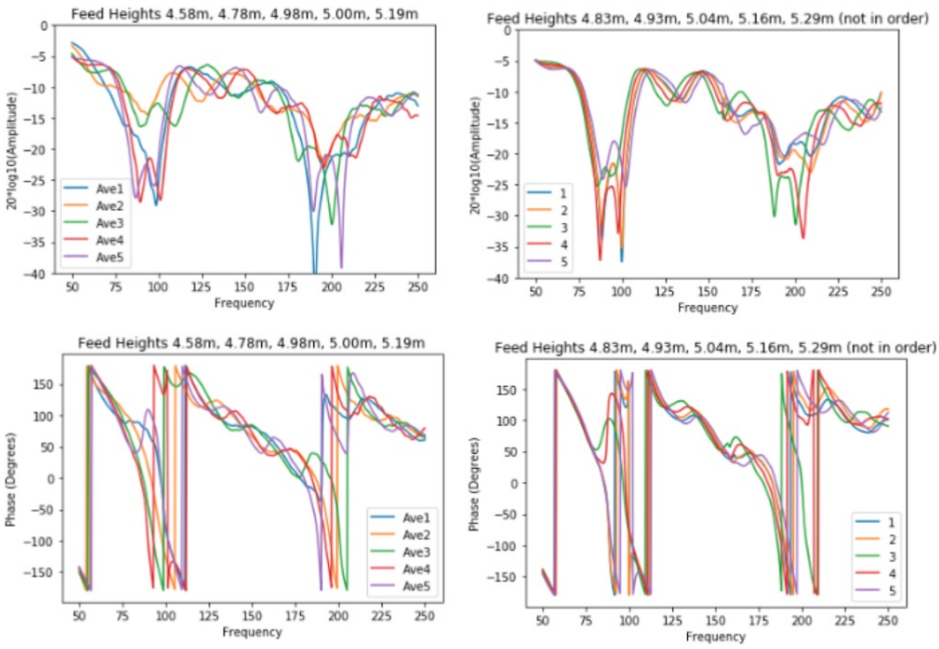

Fig. 4.— Measured S11 amplitudes and phases for the different heights of the feed above the dish. Left: data taken in July 2018. Right: data taken in September 2018.

3. Electromagnetic Models

Electromagnetic modeling was carried out using the CST Microwave Studio electromagnetic modeling software package[1]. Three models for the HERA Phase II dish+feed combination were developed, all based on the the model of Fagnoni et al. (2021), and discussed in more detail by Nhan et al. (URSI 2021) and Nahn et al. (memo in preparation): (1) The Fagnoni et al. "detailed" model, originally implemented in the 2016 version of CST, was modified to run on the 2020 version of CST; (2) a "simplified" HERA antenna model was created by removing the screw mounting holes, cables, the front-end module (FEM), and mounting hardware; (3) and a "simplified+FEM" model was created by adding the FEM back into the simplified model. Figure 5 shows a diagram of the model for the feed.

[1]http:/www.3ds.com/products-services/simulia/products/cst-studio-suite

We note that the presence or absence of the FEM, a metallic structure of size comparable to structures in the feed in the nearfield region, might be expected to affect the results of the modeling. In Figure 6 we display the S11 amplitudes and phases for the three electromagnetic models. There are significant differences in S11 amplitude and phase between the three models, particularly at the higher frequencies. Extensive modeling of feed motion, including variations in position and tilt, are in progress and will be reported elsewhere. In this memo we focus on a sequence of models with feed motion in the vertical direction, and we compare the agreement between measurement and model for two of the models, the detailed and simplified models.

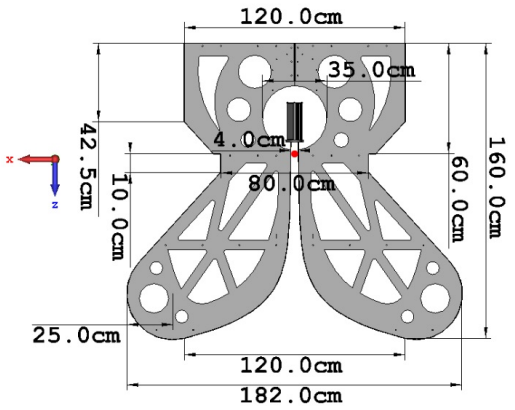

Fig. 5.— A diagram of the CST feed model (reproduced from Fagnoni et al., 2021). The reference point for the fiducial feed height of 5m is marked by the red dot.

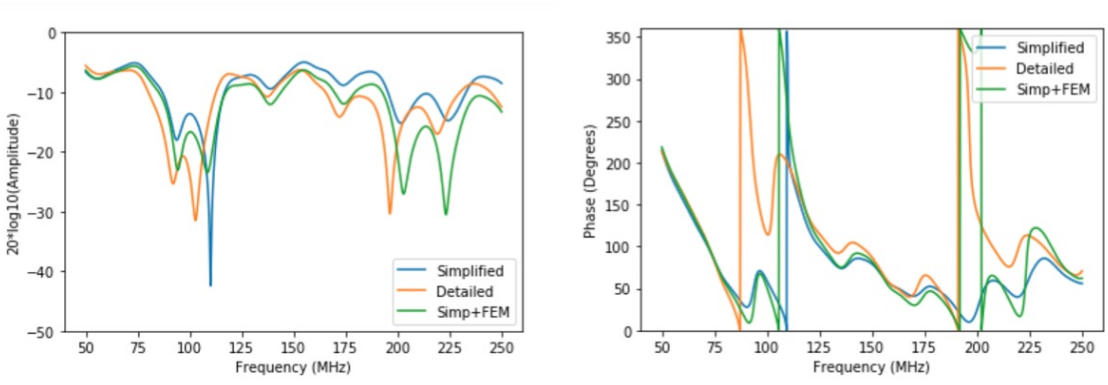

Fig. 6.— A comparison of S11 amplitudes and phases for the three electromagnetic models. The height of the feed above the dish is 5.00m for all three.

For the simplified model, CST calculations of S11 were carried out for heights of -50cm, -45cm, -40cm, -35cm, -30cm, -25cm, -20cm, -15cm, -10cm, -5cm, 0cm, 5cm, 10cm, 15cm, 20cm, 25cm and 30cm relative to the fiducial feed position. For the detailed model, CST calculations of S11 were carried out for heights of -42cm, -22cm, -17cm, -7cm, -4cm, 0cm, 4cm, 16cm, 19cm, and 29cm relative to the fiducial feed position. For both sets of models, the real and imaginary components of S11 at these values of the height were interpolated, using a cubic spline,[2] onto a grid that spanned the range of heights modeled, and was sampled with a resolution of 1cm. The interpolated S_{11} quantities are plotted in Figure 7. The functions appear to change smoothly with feed height, and the interpolations do not appear to have any numerical artifacts. We experimented also with polynomial fitting and resampling to the grid; this did not significantly change the results.

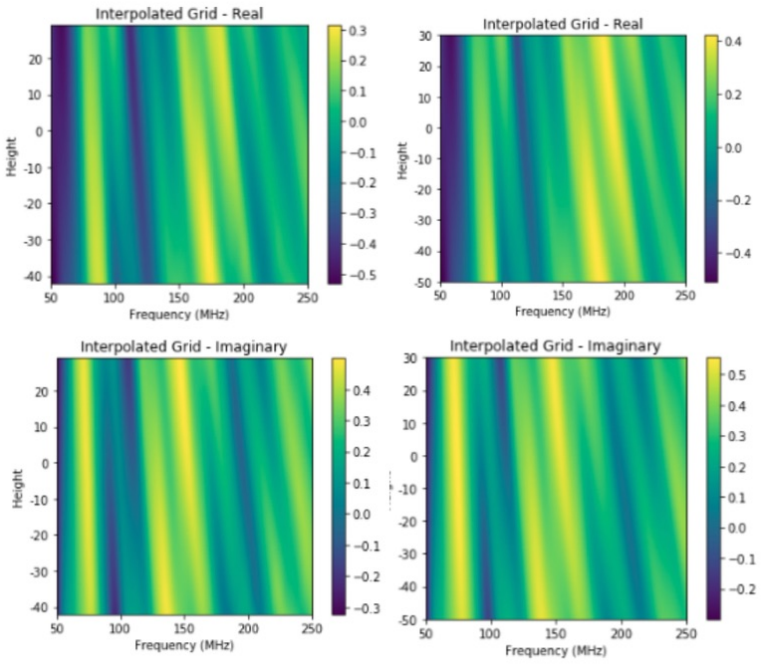

Fig. 7.— Real and imaginary parts of modeled S11, interpolated onto a grid that spans the range of heights of the feed. Left: Detailed model. Right: Simplified model. The units are linear.

[2]scipy.interpolate CubicSpline

4. Comparisons of Measured and Modeled S11

To compare the measured (data) and modeled S11, we compute the following statistic

$$\chi^2 = \sum_{i=1}^{N} \left[\frac{(\mathrm{Re}(\mathrm{S}_{11,\mathrm{m}}) - \mathrm{Re}(\mathrm{S}_{11,\mathrm{d}}))^2}{\sigma_o^2/N_{\mathrm{ave}}} + \frac{(\mathrm{Im}(\mathrm{S}_{11,\mathrm{m}}) - \mathrm{Im}(\mathrm{S}_{11,\mathrm{d}}))^2}{\sigma_o^2/N_{\mathrm{ave}}} \right] \quad (1)$$

where "m" and "d" refer to the model and the data, respectively, N_{ave} is the number of S_{11} measurements averaged together, and σ_o is the error on one measurement described in Section 2. In the presence of gaussian measurement errors, this statistic should have a χ^2 distribution. Our field measurements of height come with considerable uncertainty, probably at the level of one to a few centimeters. Therefore, for each feed height measurement, we allowed the model height to be a free parameter, and we computed the χ^2 statistic as a function of the model height. We did this calculation for the two sets of measurements and the two models, resulting in the four panels of results presented in Figure 8 (for the September measurements) and Figure 9 (for the July measurements). For the July measurements, we restrict the comparison to those data for which the set height is known and within the range of the heights in the models. For both sets of measurements, the detailed CST model is a better fit to the data than the simplified CST model. The detailed model better reproduces the S11 behavior of the data, and only the detailed CST model has values of the reduced χ^2 that are smaller than 5. As noted above, we have *a priori* reason to believe that the detailed model, with its inclusion of more structures that we know are part of the antenna element, is a better model. The S_{11} measurements appear to confirm this. Therefore, this exercise suggests that S_{11} measurements can be used to discriminate between different models of the HERA antenna elements.

5. The Best-Fit Heights

The S11's clearly change significantly with different heights of the feed, and an interesting question is whether measurements of S11 could be used to determine the heights. Since the simplified model is not a good fit to the data, we consider just the detailed model in this section. Table 2 compares the set height, the fitted height, and the difference for each measurement. Differences range from 4cm to 7cm for the September data, and they are 9cm and 11cm for the July data. The first author of this memo is of the opinion that it is entirely possible that the reference points for the two experiments were registered differently at the level of about 5cm. The results of the fitting exercise all place the best-fit antenna height *above* the measured height.

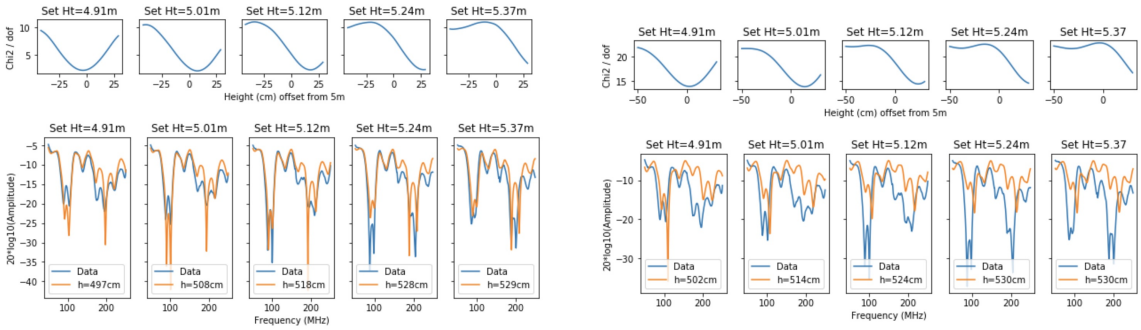

Fig. 8.— Comparison of the September data to the detailed model (left) and the simplified model (right). The top row shows the reduced χ^2 statistic as a function of the modeled feed height. We take the best-fit height to be the value of the height at the minimum. The second row shows the measured S_{11} as a function of frequency (blue) and the S_{11} for the model that assumes the best-fit height, also as a function of frequency.

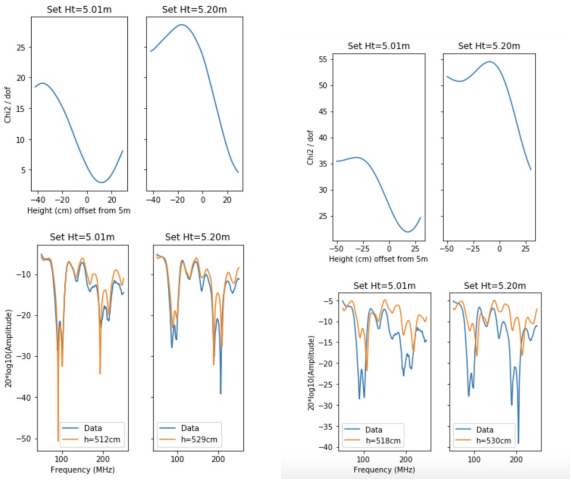

Fig. 9.— Comparison of the July data to the detailed model (left) and the simplified model (right). The data and models are displayed in the same way as Figure 8.

6. Prediction of Antenna Autocorrelation Spectra

We follow the derivation of Fagnoni et al. 2020 to predict the response of the antenna-receiver system to an incoming electromagnetic wave, referring to Figure 10. We seek to derive the response of the system, V_2, to an incident electromagnetic wave, $\mathbf{E}_{\text{in}}$. This fre-

Label	Set Height (m)	Fitted Height (m)	Difference (m)
S1	4.91	4.97	0.06
S2	5.01	5.08	0.07
J4	5.01	5.12	0.11
S3	5.12	5.18	0.06
J5	5.20	5.29	0.09
S4	5.24	5.28	0.04
S5	5.37	> 5.29	–

Table 2: The seven feed heights for which the "set heights" (heights measured in the field, corrected to a common reference point) were within or near the range simulated in the electromagnetic modeling. The "fitted height" is the best-fit height in the data-model comparison; for the S5 comparison the minimum appears to be just outside the range modeled. For the labeling, "J" refers to a measurement taken in July, and "S" refers to a measurement taken in September.

quency and angle dependent response is $\mathbf{H}(\nu, \theta, \phi)$ defined by

$$V_2(\nu, \theta, \phi) = \mathbf{H}(\nu, \theta, \phi) \cdot \mathbf{E}_{\rm in}(\nu, \theta, \phi) \tag{2}$$

and like the effective length of the antenna $\mathbf{h}(\nu, \theta, \phi)$, the quantity that links the amplitude and direction of an incoming electromagnetic wave vector to the voltage at the antenna terminals, $\mathbf{H}(\nu, \theta, \phi)$ has units of length. The open-circuit voltage at the antenna terminals can be treated like that of a generator, with internal impedance $Z_{\rm ant}$, delivering the voltage $V_{\rm oc}$:

$$V_1(\nu, \theta, \phi) = V_{\rm oc}(\nu, \theta, \phi) = \mathbf{h}(\nu, \theta, \phi) \cdot \mathbf{E}_{\rm in}(\nu, \theta, \phi) \tag{3}$$

The effective length of the antenna is the same in transmission and reception according to reciprocity principle. We use electromagnetic modeling of transmission by the antenna to determine a model voltage beam pattern $\mathbf{E}_{\rm pat}$ (units are Volts/meter), and this is related to the effective length by (see Orfanidis 2016, Chapter 16):

$$\mathbf{h}(\nu, \theta, \phi) = -\mathbf{E}_{\rm pat}(\nu, \theta, \phi) \frac{4\pi r}{k Z_{\rm fs} I_{\rm fp}(\nu)} j \tag{4}$$

where $k = 2\pi/\lambda$ is the amplitude of the wave vector, $Z_{\rm fs} = 377\ \Omega$ is the free space impedance, and $I_{\rm fp}(\nu)$ is the current at the feed point (note that $\mathbf{E}_{\rm pat}$ drops off as $1/r$, so $\mathbf{h}$ has no dependence on r).

We determine the effective length in electromagnetic modeling by simulating the antenna in transmission, excited by the current $I_{\rm fp}(\nu)$ at the feed point. The power wave associated

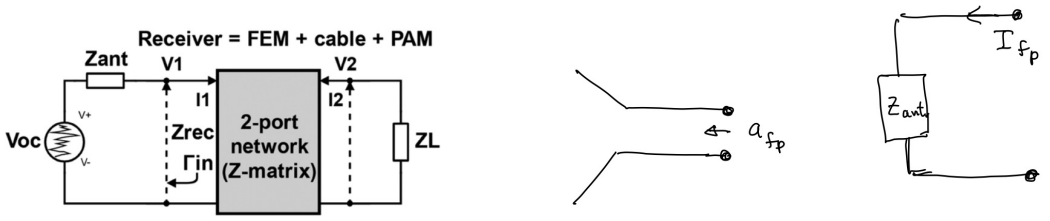

Fig. 10.— Left: (Figure 3 of Fagnoni et al. 2020): Equivalent electrical circuit of the antenna-RF receiver system. Center: Power wave incident at the feed point for the electromagnetic modeling. Right: Current at the feed point for the electromagnetic modeling.

with the current that excites the antenna at the feed point has amplitude

$$a_{\rm fp}(\nu) = \frac{V_{\rm fp}(\nu) + Z_o I_{\rm fp}(\nu)}{2\sqrt{Z_o}} \tag{5}$$

Here, $Z_L = Z_o = 100\ \Omega$, appropriate for a differential mode signal traveling on 50-Ω cables and we have $V_{\rm fp} = I_{\rm fp} Z_{\rm ant}$ (see Figure 10). Therefore, we can express the current at the feed point in terms of the amplitude:

$$I_{\rm fp}(\nu) = \frac{2\sqrt{Z_o} a_{\rm fp}(\nu)}{Z_{\rm ant}(\nu) + Z_o} \tag{6}$$

Substituting into Equation 4 gives

$$\mathbf{h}(\nu, \theta, \phi) = -\frac{2\pi}{k Z_{\rm fs}} j \frac{Z_{\rm ant}(\nu) + Z_o}{\sqrt{Z_o} a_{\rm fp}(\nu)} \mathbf{E}_{\rm pat}(\nu, \theta, \phi) \tag{7}$$

The magnitude of the simulated antenna pattern at each frequency will scale with the input signal amplitude $a_{\rm fp}(\nu)$ and with the distance r from the antenna; the CST software corrects for the variation of $a_{\rm fp}(\nu)$ with frequency and outputs the beam pattern at a fiducial distance. For our study of the dependence of the antenna autocorrelation on frequency, we are not interested in the overall amplitude of the signal. However, the antenna impedance and the complex beam pattern are both functions of frequency. Therefore, we define a normalized version of the antenna effective length that captures all the frequency dependence of the antenna effective length but has an arbitrary overall amplitude:

$$\mathbf{h}_o(\nu, \theta, \phi) = -\frac{Z_{\rm ant}(\nu) + Z_o}{\nu \sqrt{Z_o}} \mathbf{E}_{\rm pat}(\nu, \theta, \phi) \tag{8}$$

Finally, we use the relationship between $V_{\rm oc}$ and V_2 (assuming $Z_L = Z_o$)

$$V_2(\nu) = V_{\rm oc}(\nu)\left[\frac{Z_o Z_{r21}(\nu)}{(Z_o + Z_{r22}(\nu))(Z_{\rm ant}(\nu) + Z_{r11}(\nu) - Z_{r21}(\nu)Z_{r12}(\nu)}\right] \tag{9}$$

to write $\mathbf{H}_o = V_2\mathbf{h}_0/V_{\rm oc}$ as

$$\mathbf{H}_o(\nu,\theta,\phi) = -\mathbf{E}_{\rm pat}(\nu,\theta,\phi)\left[\frac{Z_{\rm ant}(\nu)+Z_o}{\nu\sqrt{Z_o}}\right]\left[\frac{Z_o Z_{r21}(\nu)}{(Z_o + Z_{r22}(\nu))(Z_{\rm ant}(\nu) + Z_{r11}(\nu)) - Z_{r21}(\nu)Z_{r12}(\nu)}\right] \tag{10}$$

where the subscript r denotes to the impedance of the receiver, which in our case includes the HERA FEM and PAM.

Data on the receiver scattering parameters have been kindly made available by E. de Lera Acedo[3]. To use these data to determine $\mathbf{H}_o$, we can rewrite the last term in brackets in terms of the scattering parameter S_{21} relating a wave incident on the 2-port network. For a linear two-port network, the impedance matrix is defined by

$$\begin{bmatrix} V_1 \\ V_2 \end{bmatrix} = \begin{bmatrix} Z_{11} Z_{12} \\ Z_{21} Z_{22} \end{bmatrix} \begin{bmatrix} I_1 \\ I_2 \end{bmatrix} \tag{11}$$

and the scattering matrix is defined by

$$\begin{bmatrix} b_1 \\ b_2 \end{bmatrix} = \begin{bmatrix} S_{11} S_{12} \\ S_{21} S_{22} \end{bmatrix} \begin{bmatrix} a_1 \\ a_2 \end{bmatrix} \tag{12}$$

where a_i and b_i are the incoming and outgoing power waves for the ith port. The relationship between the impedance matrix and the scattering matrix is

$$\mathbf{S} = (\mathbf{Z} - Z_o\mathbf{I})(\mathbf{Z} + Z_o\mathbf{I})^{-1} \tag{13}$$

$$\mathbf{Z} = (\mathbf{I} - \mathbf{S})^{-1}(\mathbf{I} + \mathbf{S})Z_o \tag{14}$$

where $\mathbf{I}$ is the identity matrix (see, for example, Orfanidis (2016), Chapter 14). We need the matrix element S_{21} which is

$$S_{21} = \frac{2Z_{21}Z_o}{(Z_{11} + Z_o)(Z_{22} + Z_o) - Z_{12}Z_{21}} \tag{15}$$

Substituting this into the expression for $\mathbf{H}_o$ we have

$$\mathbf{H}_o(\nu,\theta,\phi) = \frac{Z_{\rm ant}(\nu) + Z_o}{\nu\sqrt{Z_o}}\mathbf{E}_{\rm pat}(\nu,\theta,\phi)S_{r21} \tag{16}$$

[3]http://git.mrao.cam.ac.uk/shc44/HERA-RF/-/tree/master/RF_tests

where S_{r21} is an element of the scattering matrix that relates the power wave amplitude incident on the receiver to the power wave amplitude leaving the receiver.

Equation 18 can also derived by considering the power wave incident at the antenna terminals, and propagating it through to the output of the receiver.

The elements of the 3×3 scattering matrix for FEM233_PAM233_E are plotted in Figure 11. Port 2 is the output port; single-ended ports 1 and 3 must be combined to form the differential input port giving:

$$S_{r21} \equiv S_{21sd} = \frac{1}{\sqrt{2}} \left[S_{21ss} - S_{23ss} \right] \tag{17}$$

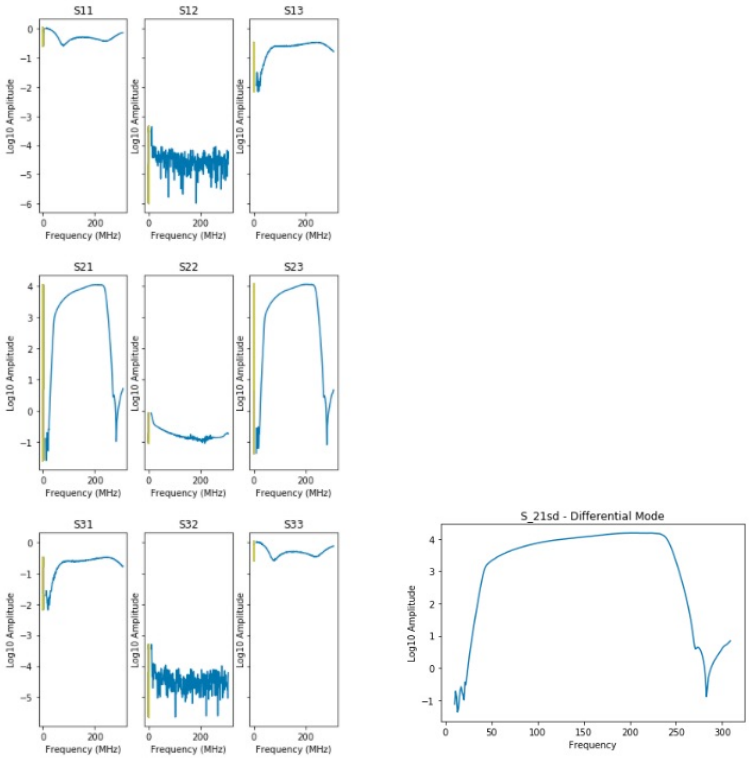

Fig. 11.— Left: Measured scattering parameters of FEM233_PAM233_E. Right: $S_{r21}(\nu)$ (see Equation 17).

To predict the frequency dependence of uncalibrated autocorrelation of an antenna from the CST-modeled S_{11} of the antenna we need to integrate the sky brightness weighted by the antenna pattern. However, if the sky brightness is dominated by a bright source at boresight,

the response can be approximated by

$$\mathbf{H}_o(\nu, 0, 0) = \frac{Z_{\rm ant}(\nu) + Z_o}{\nu\sqrt{Z_o}} \mathbf{E}_{\rm pat}(\nu, 0, 0) S_{r21}(\nu) \tag{18}$$

We have combined the antenna impedances given by the CST models, the frequency dependence of the antenna gain at boresight given by the CST models, and the S_{r21} scattering parameter inferred from measurements to compute the response of the antenna-receiver system. The results are shown in Figure 12. We also show measurements of HERA antenna autocorrelation spectra (reproduced from Dynes et al. 2019). The autocorrelation spectra were taken with the array pointing at galactic coordinates $(\ell, b) = (309°, 32.5°)$, and the spectra represent the convolution of the sky brightness at that point convolved with the antenna beam, propagated through the system response. We do not expect the detailed features of the response function to match the measured spectra, because we do not have a model that gives the scattering parameters for an antenna placed in an array (and we have seen in Section 4 that the S_{11} scattering parameter is sensitive to details of the antenna construction). However, in both the model and the data, features in the spectrum move to the left (lower frequency) as the feed is raised. This is expected, because as the feed is raised standing waves between the feed and the dish will have a longer wavelength. Also, the magnitude of the frequency drift of features with feed height is larger at higher frequencies. This is also expected, because at higher frequencies a given motion of the feed is a larger fraction of the wavelength. It appears that the changes of the autocorrelation spectra with feed height are systematic, and in principle could be predicted with an accurate antenna model. In the absence of such a model, the response could be calibrated with measurements of autocorrelation spectra with the feed at different heights.

7. Summary

Three electromagnetic models for the (isolated, not in an array) HERA antenna element that differ in the degree to which they include components of the real antenna give significantly different predictions for the scattering parameter S_{11} as a function of frequency. In a comparison of two of the models to S_{11} data measured in the field, the one that more closely reproduces the as-built antenna (i.e., the "detailed model" of Fagnoni et al.) is clearly a better fit to the data. This suggests that one should seek agreement between modeled and measured S_{11} when evaluating the fidelity of an electromagnetic model, and that the sensitivity of the S_{11} parameter to details of the antenna construction make it a good discriminator between models.

Physically measuring feed heights in the field is cumbersome and prone to error, so we

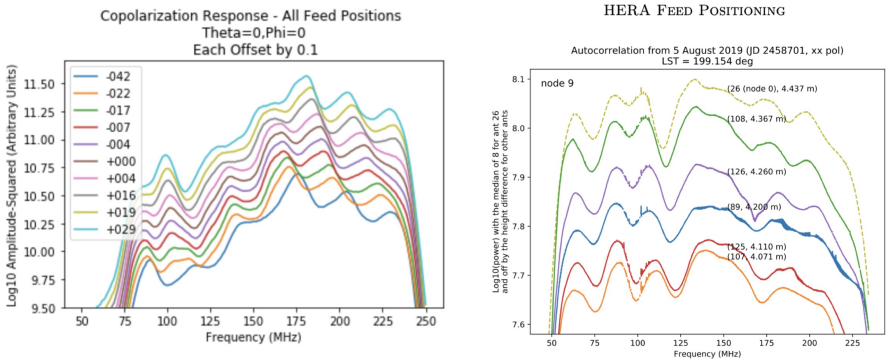

Fig. 12.— Left: Modeled antenna-feed system reponse as a function of frequency (see Equation 18). Right: Field measurements of autocorrelation for different feed heights.

explored whether S_{11} measurements might be used to determine feed height. This could be useful in data analysis (for example, for selecting from a library of antenna models) or in operations (for example, for determining whether the height of a feed needs to be adjusted). Electromagnetic models that reproduce the detailed model of Fagnoni et al, except for variations in the feed height, predict significant differences in the behavior of S_{11} versus frequency for different feed heights. We formed an interpolated grid of a set of the models, and found the best-fit height for each measurement of S_{11}.

The best fit heights were found to be consistently larger than the height measured in the field, at the level of at least a few centimeters. It is possible that the determination of the position of antenna vertex in the field was in error by this amount. An alternative possibility is that the model does not exactly reproduce the performance of the antenna (the fits are not perfect, after all), and the data-model comparison produces a biased estimator of the feed height. A third possibility is that, in addition to the motion in the vertical direction modeled, there was feed motion in the horizontal direction and/or tilt that is biasing the estimate of height. The scatter within each group of measurements suggests that the model-data comparison procedure presented here could be capable of determining feed position with a precision of about 2cm, if the source of the bias could be understood.

Measurements of S_{11} produce radio frequency interference, so it may not be practical to carry out such measurements during periods of science operations. Therefore, we modeled the response of the antenna-feed system by combining the modeled antenna impedance, the modeled antenna beam pattern, and measurements of the receiver scattering parameters. When combined with a model of the sky, this response in principle gives a prediction of

the antenna autocorrelation function. Since we do not have a detailed model of the HERA antenna embedded in an array we are unable to do this prediction for the HERA autocorrelation spectra. However, we find qualitative agreement between the the modeled system response and data taken in the field. We believe it is safe to conclude that the autocorrelation spectra vary systematically with feed height, and that the relationship could be calibrated with measurements taken as the feed height is varied.

Further modeling of feed motion, that includes horizontal motion and tilt, is in progress. We plan to explore whether including these degrees of freedom in the modeling improves the agreement of the measurements and models. We also would like to explore whether observations made with the Galactic center in the primary beam might have sufficient signal-to-noise to enable determination of feed height from measurement of the antenna autocorrelation spectrum.

8. Acknowledgements

We thank Honggeun Kim and Nicholas Kern for very helpful discussions. We further thank Honggeun Kim for carrying out the electromagnetic models for the “simplified” model of the dish-feed system.

REFERENCES

de Lera Acedo, E., Bolli, P., Paonesssa, F., et al., "SKA Aperture Array Verification System: Electromagnetic Modeling and Beam Pattern Measurements Using a Micro UAV." 2018, Experimental Astronomy.

Dynes, S. B. C., Josaitis, A. T., de Lera Acedo, E., et al., "Vivaldi Feed Positioning: Tests, Implementation, and Results." HERA Memo #75, reionization.org.

Fagnoni, N., de Lera Acedo, E., Drought, N., et al., "Design of the New Wideband Vivaldi Feed for the HERA Radio-Telescope Phase II," 2021, IEEE Transactions on Antennas and Propagation.

Fagnoni, N., de Lera Acedo, E., DeBoer, D., et al., "Understanding the HERA Phase I Receiver System with Simulations and its Impact on the Detectability of the EoR Delay Power Spectrum." 2020, MNRAS.

Jacobs, D., Burba, J., Bowman, J., et al.. "First Demonstration of ECHO: an External Calibrator for Hydrogen Observatories." 2017, Publications of the Astronomical Society of the Pacific.

Nhan, B., "HERA's Vivaldi Feed VNA Measurement Follow-up at GBO." 2018, Unpublished memo.

Neben, A., Bradley, R., Hewitt, J., et al, "The Hydrogen Epoch of Reionization Array Dish: I. Beam Pattern Measurements and Science Implications, 2016, The Astrophysical Journal.

Orfinidis, S. *Electromagnetic Waves and Antennas*, 2016,
https://www.ece.rutgers.edu/~orfanidi/ewa/

Nunhokee, C., Parsons, A., Kern, N., et al., "Measuring HERA's Primary Beam in Situ: Methodology and First Results." 2020, The Astrophysical Journal.